Comparative antibacterial activity of *Psoralea corylifolia* seed extract – mediated titanium dioxide and zinc oxide nano particles

Badugu Emmanuel [1,2] Prof.M.E.Rani*

[1]Research Scholar, Department of Chemistry, Rayalaseema University, Kurnool-518007, AP, India.
[2]Department of Chemistry, Rajiv Gandhi University of Knowledge and Technologies. Rkvalley, Kadapa-516330, AP, India.
*Professor, Department of Chemistry, Rayalaseema University, Kurnool-518007, AP, India.

Abstract:

The green synthesis method provides stable, rapid, and eco-friendly methods for synthesis nano particles with plant extract as capping and reducing agents. This method renders to determine the synthesis, characterization and the antibacterial potential of Titanium dioxide nanoparticles(TiO_2NPs) and Zinc oxide nanoparticles(ZnONPs) by using psoralea corylifolia seed extract.The Nanoparticles were characterized by UV–Vis spectrophotometry, Fourier transform infrared (FTIR) spectroscopy, scanning electron microscopy (SEM).Antibacterial potential of nanoparticles is analysed by standard disc diffusion method against bacterial strains including Escherichia coli, Pseudomonas aeruginosa, Staphylococcus aureus, and Bacillus subtilis.The maximum zone of inhibition is observed for Staphylococcus aureus and Pseudomonas aeruginosa against TiO_2 and ZnO NPs respectively, at different concentration of NPs. The susceptibility of NPs against bacterial strains is evaluated in the E. coli and Bacillus subtilis showed moderate inhibition zones with both NPs. Results revealed that ZnO NPs have more antibacterial activity in contrast to TiO_2 NPs.

Keywords: Psoralea corylifolia seed extract, Titanium dioxide nano particles, Zinc oxide nanoparticles, Comparative antibacterial activity.

Introduction:

In recent years, there has been a growing interest among researchers in green chemistry for the synthesis of NPs using environmentally friendly agents. These agents significant research has been conducted on the use of plant extracts for NP synthesis, revealing that plants are particularly well-suited for NP production, even at the pilot scale (1,2,3,5). Zinc oxide (ZnO) (9,10,14) and titanium dioxide (TiO_2) (5,6,7) nanoparticles (NPs) have garnered significant interest in the scientific community due to their unique biological, chemical, and physical properties, high surface-to-volume ratio, and the availability of more surface atoms for immediate chemical reactions (7,8,10,11). These compounds have attracted the attention of numerous researchers because of their diverse range of applications. In the next section, we will delve into the schematic illustration of green synthesis approaches and characterization and their antibacterial activity (6,7,11,15) for ZnO and TiO_2 nanostructures. The zinc oxide is showing higher reactivity than titanium dioxide nanoparticles (16,17,19,20).

Materials and methods:

Sample collection & Preparation of the Psoralea corylifolia seed powder :

The seeds of were procured from an authenticated ayurvedic shop, proddatur. It was taxonomically authenticated by Dr. Uma Maheshwari, Department of Biology, Rajiv Gandhi University of Knowledge and Technologies. Rkvalley, Kadapa. And the seeds are crushed and grinded with the 750-watt Preethi zodiac mixer with smooth operation to get the powder form. The collected powder was stored in airtight container at room temperature until further use and the chemicals were received from the sisco research laboratories Pvt.Ltd (SRL) and are used without any purification.

Biosynthesis of Psoralea corylifolia seed extract with Ethanolic solution TiO_2 & ZnO NPs:

The 30 grams of powdered seed is soxlated with 400mL ethanol and it is stored and is used for further analysis. The psoralea corylifolia seed extract with ethanolic solution is utilized for the titanium dioxide and zinc oxide nano particles synthesis. 3mL of plant seed extract was placed and into conical flask and 50mM TiO_2 with 1% alcoholic KOH and the appeared colour is light brownish honey like colour. And then another conical flask with 3mL plant seed extract and 50mM ZnO with 1% alcoholic KOH and the appeared colour is dark brownish. The biosynthesized titanium dioxide and zinc oxide NPs solutions were further analysed for UV, FTIR, SEM & EDS and their antibacterial activity.

a) seeds of psoralea corylifolia, b) seed powder, c) soxlate extraction, d) seed extract

d)psoralea corylifolia seed extract, e) TiO_2 NPs, f) Biosynthesized TiO_2 NPs

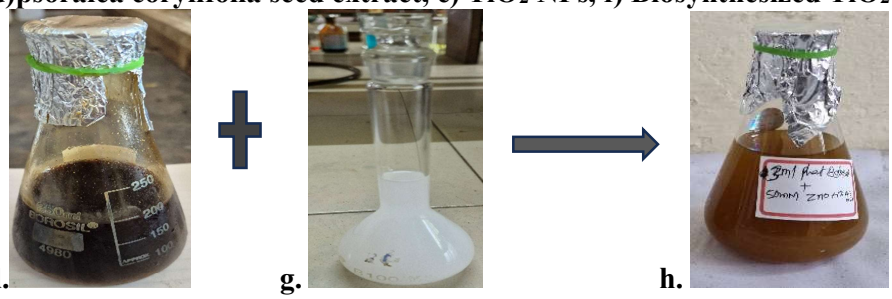

d) psoralea corylifolia seed extract g) ZnO NPs, h) Biosynthesized ZnO NPs

Results and discussion:

UV–Visible Spectroscopic Analysis:

The UV–Vis spectrum of TiO_2 nanoparticles reveals a prominent absorption peak at 372 nm, which corresponds to an optical band gap of approximately 3.33 eV, indicating the presence of the anatase

crystalline phase (approx. 360-380nm) and nanoscale dimensions. The adsorption edge at 372nm corresponds to the band gap transition of titanium dioxide nanoparticles and UV absorption due to Ti–O charge transfer. The observed blue shift in comparison to bulk titanium dioxide provides confirmation of quantum confinement, while the significant UV absorbance highlights the exceptional potential for UV driven photocatalytic and antibacterial application. Furthermore, the gradual decrease in absorbance beyond 400 nm serves as confirmation of the UV-active nature of the synthesized titanium dioxide nanoparticles.The UV-Vis spectrum displays a distinct excitonic absorption peak at 361 nm, which validates the formation of ZnO nanoparticles with a bandgap of approximately 3.43 eV. The observed blue shift, in comparison to bulk ZnO, indicates that quantum confinement is at play due to the nanoscale size of the particles with a high degree of crystallinity. The strong UV absorption demonstrates that the ZnO NPs are UV-active semiconductors, capable of generating reactive oxygen species, making them excellent candidates for photocatalytic and antibacterial applications. The higher band gap compared to titanium dioxide indicates smaller particle size and stronger quantum confinement effects.

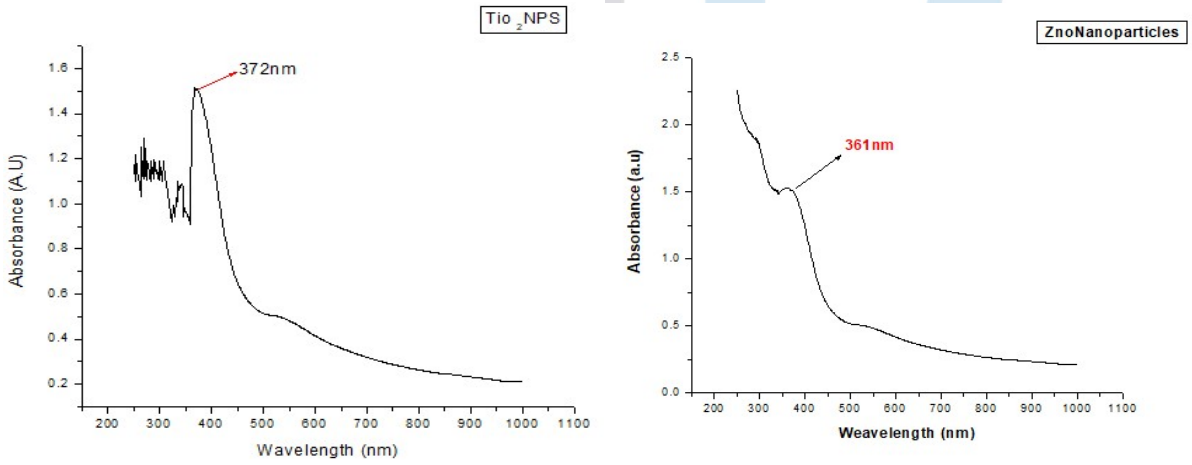

Fig.1- UV spectra of TiO_2 NPs & ZnO NPs

Fourier Transform Infrared Spectroscopic Analysis (FTIR):

In Fig:2a the FTIR peaks observed at 3349, 1740, 1640, 1370, and 1215 cm^{-1} for TiO_2 nanoparticles signify the existence of various functional groups linked to synthesis or surface modification processes: The peak around 3349 cm^{-1} is associated with the stretching vibration of O–H or N–H groups, indicating the presence of surface hydroxyl groups or amines. This occurrence is typical for TiO_2 nanoparticles due to the adsorption of water or the presence of amine capping agents. The peak at 1740 cm^{-1} is generally ascribed to C=O stretching vibrations, which denote the presence of carbonyl groups such as carboxylic acids, acid anhydrides, or lactones derived from organic precursors or residual solvents.

The peak at 1640 cm^{-1} is frequently attributed to bending vibrations of molecular water (H–O–H bending), although it may also suggest the presence of C=C stretching in alkenes. The peak at 1370 cm^{-1} is typically due to phenols (C–O stretching) or the bending vibration of methyl (CH_3) or carboxylate groups. The peak at 1215 cm^{-1} may correspond to C–O stretching in ethers or phenols, indicating organic groups that remain from synthesis reagents or capping agents. These FTIR signatures imply that the TiO_2 nanoparticles are

likely to possess surface functional groups resulting from synthesis or capping processes, which are commonly observed in green or sol–gel mediated nanoparticle preparations.

In Fig:2b the FTIR peaks observed at 3350, 2973, 1741, and 1046 cm^{-1} in ZnO nanoparticles signify the existence of particular functional groups linked to their synthesis and surface chemistry: The peak near 3350 cm^{-1} is ascribed to the stretching vibration of O–H groups from hydroxyl compounds or adsorbed water, which are typically present on the surfaces of ZnO nanoparticles. The peak around 2973 cm^{-1} is related to C–H stretching vibrations, indicating the presence of aliphatic organic groups or residual capping/templating agents from the synthesis process. The peak at approximately 1741 cm^{-1} denotes the stretching vibration of C=O groups (carbonyl), implying the presence of aldehydes, ketones, or carboxylic acids derived from organic precursors or surface modifications. The peak at about 1046 cm^{-1} is linked to either C–O stretching vibrations (from primary alcohols or ethers) or C–N stretching (from amines), which may stem from precursors or biopolymer stabilizers utilized during synthesis. These FTIR characteristics collectively suggest that the ZnO nanoparticles exhibit surface hydroxyl, carbonyl, alkyl (C–H), and alcohol or amine functionalities, which are typical of green or chemically-assisted nanoparticle fabrication.

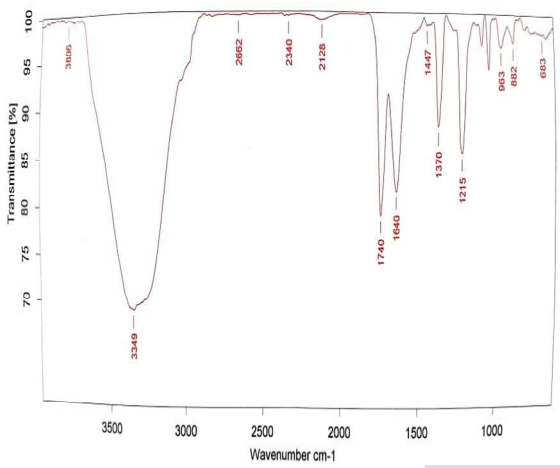

Fig. 2a- FTIR spectra of TiO_2 NPs

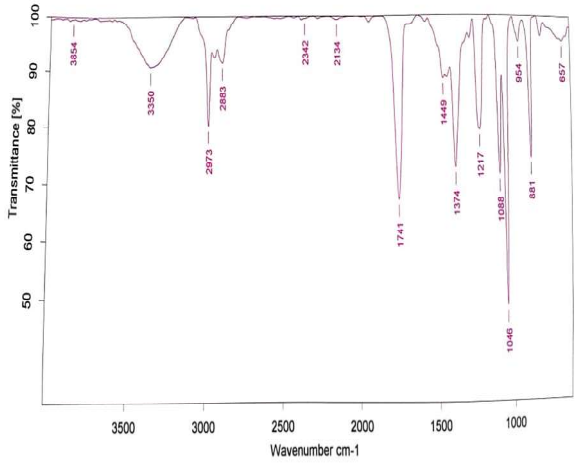

Fig. 2b- FTIR spectra of ZnO NPs

X-ray Diffraction (XRD):

XRD pattern shows sharp and intense peaks at specific 2θ values. In the titanium dioxide NPs FTIR graph the relative intensity (approx.) peaks at 25.3 with 100% and 48.0 with 55% and the XRD pattern corresponds to Anatase (tetragonal) TiO_2 nanoparticles, with the main diffraction peaks and their corresponding Miller indices as 25.3(101), 37.8(004), 48.0(200), 54.0(105), 62.7(204), 68.8(116) values. In the zinc oxide NPs FTIR graph the relative intensity (approx.) peaks at 36.2 with 100% and 34.4 with 80%, 31.7 with 60% and with the main diffraction peaks and their corresponding Miller indices as 31.7(100), 34.4(002), 36.2(101),47.5(102) are high crystallinity and narrow peaks indicate well-defined, nanocrystalline grains. 20–40 nm range, assuming moderate peak broadening typical for ZnO nanoparticles. Comparing XRD peaks visually the positions and intensities align closely with this wurtzite ZnO pattern confirming the phase purity.

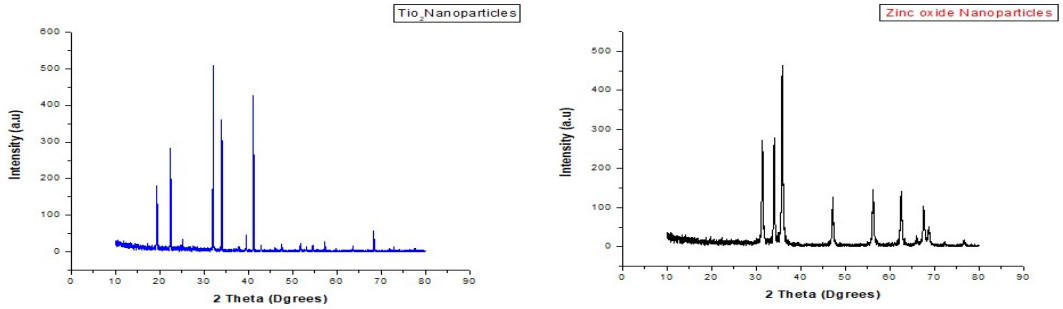

Fig. 3 – XRD diffractogram of TiO_2 NPs & ZnO NPs

Scanning Electron Microscope (SEM):

TiO_2 NPs:

The morphology and particle size of the synthesized TiO_2 nanoparticles were analysed using scanning electron microscopy (SEM). The images showed that the particles predominantly displayed spherical to polyhedral shapes, with sizes ranging from about 171 to 347 nm. The smaller particles, measuring 171–215 nm, had relatively smooth surfaces and showed limited agglomeration, suggesting a consistent nucleation and growth process. In contrast, as the particle size increased to 239–347 nm, the morphology became more irregular, with noticeable agglomeration and porosity, indicating that grain growth and some level of sintering had occurred. The size distribution reflected a moderate level of polydispersity, likely due to Ostwald ripening during the synthesis. These morphological characteristics align with the standard transition from a predominantly anatase structure at smaller sizes to a mixed anatase–rutile structure at larger particle sizes.

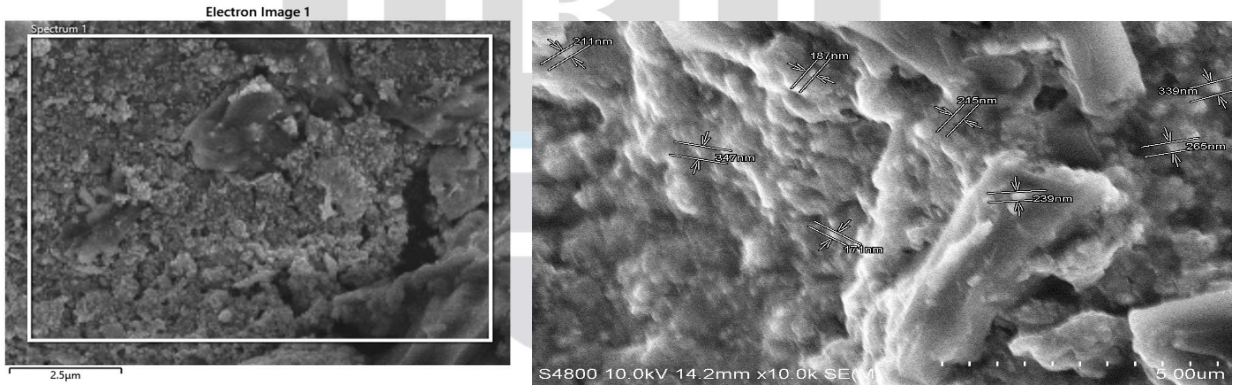

Fig. 4 SEM images of seed extract of Psoralea corylifolia TiO_2 nanoparticles

ZnO NPs:

Analysis of ZnO nanoparticles ranging from sizes of 46.3, 82.9, 84.4, 95.6, 101, 119, and 148 nm reveals the majority of the particles exhibit a spherical or nearly spherical shape, with some level of aggregation noted as the size increases due to elevated surface energy. For the smaller nanoparticles, around 46 nm, the particles appear to be more evenly dispersed with a relatively consistent morphology. In contrast, larger nanoparticles, particularly those exceeding 100 nm, tend to form clusters with less clear boundaries due to increased aggregation. In conclusion, the SEM analysis of ZnO nanoparticles within this size spectrum indicates a transition from spherical to slightly aggregated forms, with variations in dispersion and morphology that correspond closely to standard synthesis techniques.

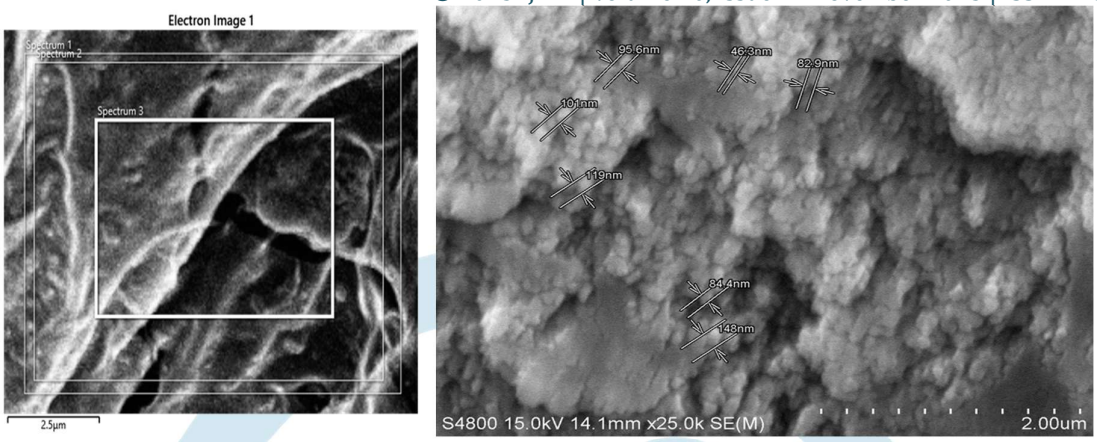

Fig. 5 SEM images of seed extract of Psoralea corylifolia ZnO nanoparticles

EDS (Energy Dispersive X-ray Spectroscopy):

The Fig.6a explains the elemental composition of the TiO_2 nanoparticles are analysed through Energy Dispersive X-ray Spectroscopy (EDS). The resulting spectrum showed a significant amount of titanium and oxygen, confirming the presence of TiO_2. The quantitative assessment indicated that titanium made up about 42.6 wt %, with a standard deviation (σ) of 13.7, hinting at some variability in composition across the studied area. The slightly lower-than-expected titanium content might be linked to oxygen enrichment on the surface, the presence of adsorbed materials, or contributions from the underlying substrate. In summary, the EDS findings support that TiO_2 is the primary phase present.

The Fig.6b explains the elemental analysis of the sample that is conducted using Energy Dispersive X-ray Spectroscopy (EDS). The results showed that zinc is a primary component, averaging about 54.9 wt%. However, the standard deviation (σ = 41.0) indicates a considerable variation in composition throughout the analysed area, suggesting that the distribution of zinc is quite uneven. This variability may stem from factors such as particle clustering, surface irregularities, or partial zinc oxidation. Additionally, the zinc content being lower than what is expected for stoichiometric ZnO suggests potential oxygen enrichment or interference from signals related to the underlying substrate. In summary, while the EDS findings confirm the presence of zinc, they also reveal significant diversity within the sample.

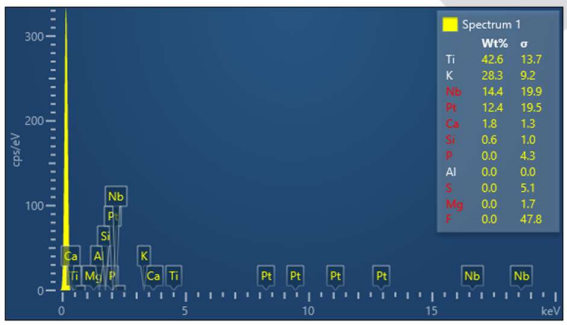

Fig. 6a) TiO_2 NPs EDS

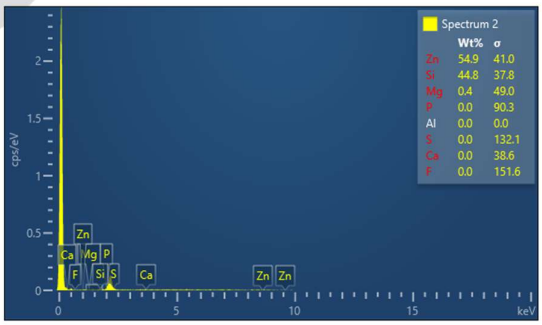

Fig. 6b) ZnO NPs EDS

Biological Application:

Antibacterial activity:

The antibacterial effectiveness of zinc oxide nanoparticles, titanium dioxide nanoparticles, and the antibiotic ampicillin was assessed using the agar well diffusion method. We obtained four bacterial strains—Escherichia coli (MTCC 443), Pseudomonas aeruginosa (MTCC 424), Staphylococcus aureus (MTCC

3160), and Bacillus subtilis (MTCC 121)—from the Microbial Type Culture Collection in Chandigarh, India. Each strain was grown in nutrient broth and incubated at 37 °C for 24 hours to promote active growth. We adjusted the bacterial suspension to match a turbidity level of 0.5 McFarland standard, which is roughly 1×10^8 CFU/mL. Next, we prepared sterile nutrient agar plates and evenly spread 100 µL of each standardized bacterial inoculum across the surface with sterile cotton swabs to create a uniform lawn. Using a sterile cork borer, we aseptically created three wells, each 6 mm in diameter, on every plate. We filled the wells with 50 µL of the test samples: titanium dioxide in the first well, zinc oxide in the second, and ampicillin (20 µg/mL) in the third as a positive control. The plates were then left at room temperature for 30 minutes to facilitate proper diffusion of the samples into the agar, followed by incubation at 37 °C for 24 hours. After incubation, we measured the zones of inhibition around each well using a digital Vernier caliper and documented the results to evaluate the antibacterial effectiveness of the compounds against each bacterial strain.

Results:

The study assessed the antibacterial properties of zinc oxide, titanium dioxide, and the standard antibiotic ampicillin against various bacterial strains, including Escherichia coli (MTCC 443), Pseudomonas aeruginosa (MTCC 424), Staphylococcus aureus (MTCC 3160), and Bacillus subtilis (MTCC 121) using the agar well diffusion method. Each of the bacterial strains exhibited distinct inhibition zones, showcasing the antimicrobial effectiveness of the tested agents. Notably, ampicillin (located in well 3) displayed the most significant inhibitory effect across all pathogens, underscoring its potent bactericidal properties. Zinc oxide (well 2) demonstrated moderate inhibition, consistently outperforming titanium dioxide (well 1) in most tests. Staphylococcus aureus and Pseudomonas aeruginosa were particularly sensitive to titanium dioxide, highlighting its promise as an antibacterial agent. In comparison, E. coli and Bacillus subtilis showed moderate inhibition zones with both zinc and titanium oxides, suggesting variability in susceptibility among different strains. Details on the quantitative measurements of the inhibition zones can be found in Table 1.

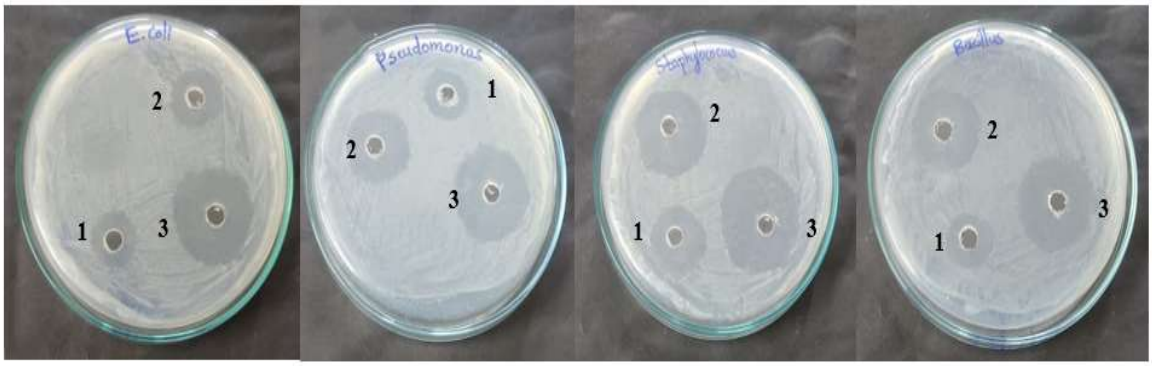

Titanium dioxide (1), Zinc oxide (2), and the standard **antibiotic ampicillin (3)**

Table 1. Zone of inhibition (mm) of different test samples against selected bacterial pathogens

Test Organism	Titanium dioxide (1)	Zinc Oxide (2)	Ampicillin (3)
Escherichia coli MTCC 443	08 ± 0.3	11 ± 0.4	18 ± 0.5
Pseudomonas aeruginosa MTCC 424	07 ± 0.4	12 ± 0.3	17 ± 0.6
Staphylococcus aureus MTCC 3160	09 ± 0.5	14 ± 0.4	19 ± 0.5
Bacillus subtilis MTCC 121	08 ± 0.4	10 ± 0.3	17 ± 0.4

Conclusions:

In this study, Psoralea corylifolia seed extract biosynthesized with the zinc oxide nanoparticles, and titanium dioxide nanoparticles via green route. The present work explains the comparative study of their UV, FTIR, XRD, and SEM analyses. The UV data shows the zinc oxide is showing higher band gap and more pronounced blue shift indicates smaller particle size relative to titanium dioxide. From the above data EDS findings confirm the presence of zinc, they also reveal significant diversity within the sample. Analysis of ZnO nanoparticles ranging from 46.3 to 148 nm reveals that antibacterial activity, surface area, and optical band gap decrease with increasing particle size, while crystallinity and stability increase. Smaller ZnO NPs (~46 nm) exhibit superior antibacterial efficacy due to enhanced ROS generation and Zn^{2+} ion release. Analysis of TiO_2 nanoparticles ranging from 171 nm to 347 nm reveals that decreasing particle size enhances optical absorption in the UV region, increases band gap energy, and significantly improves antibacterial and photocatalytic activities. Smaller TiO_2 NPs (~171 nm, anatase phase) generate more reactive oxygen species and exhibit stronger bactericidal activity than larger particles (~347 nm, mixed anatase–rutile phase). The study has established that psoralea corylifolia seed extract, biosynthesized with zinc oxide nanoparticles and titanium dioxide nanoparticles, exhibits anti-bacterial activity. It has been observed that ZnO demonstrates a higher level of reactivity compared to TiO_2.

References:

1. 1.Kumar, K.M.; Mandal, B.K.; Kumar, K.S.; Reddy, P.S.; Sreedhar, B. Biobased green method to synthesise palladium and iron nanoparticles using Terminalia chebula aqueous extract. pectrochim. Acta Part A Mol. Biomol. Spectrosc. 2013, 102, 128–133.
2. Devatha, C.P.; Thalla, A.K. Green Synthesis of Nanomaterials. Synth. Inorg. Nanomater. 2018, 169–184.
3. Benelli, G. Green Synthesis of Nanomaterials. Synth. Inorg. Nanomater. 2019, 9, 1275.
4. Subhapriya, S.; Gomathipriya, P. Green synthesis of titanium dioxide (TiO2) nanoparticles by Trigonella foenum-graecum extract and its antimicrobial properties. Microb. Pathog. 2018, 116, 215–220.
5. Nadeem, M.; Tungmunnithum, D.; Hano, C.; Abbasi, B.H.; Hashmi, S.S.; Ahmad,W.; Zahir, A. The current trends in the green syntheses of titanium oxide nanoparticles and their applications. Green Chem. Lett. Rev. 2018, 11, 492–502.
6. Kalyanasundaram, S.; Prakash, M.J. Biosynthesis and Characterization of Titanium Dioxide Nanoparticles Using Pithecellobium Dulce and Lagenaria Siceraria Aqueous Leaf Extract and Screening their Free Radical Scavenging and Antibacterial Properties.Int. Lett. Chem. Phys. Astron. 2015, 50, 80–95.

7. Bhuyan, T.; Mishra, K.; Khanuja, M.; Prasad, R.; Varma, A. Biosynthesis of zinc oxide nanoparticles from Azadirachta indica for antibacterial and photocatalytic applications. Mater. Sci. Semicond. Process. 2015, 32, 55–61.
8. Raja, A.; Ashokkumar, S.; Marthandam, R.P.; Jayachandiran, J.; Khatiwada, C.P.; Kaviyarasu, K.; Raman, R.G.; Swaminathan, M.Eco-friendly preparation of zinc oxide nanoparticles using Tabernaemontana divaricata and its photocatalytic and antimicrobial activity. J. Photochem. Photobiol. B Biol. 2018, 181, 53–58.
9. Dhanemozhi, A.C.; Rajeswari, V.; Sathyajothi, S. Green Synthesis of Zinc Oxide Nanoparticle Using Green Tea Leaf Extract for Supercapacitor Application; Elsevier: Amsterdam, The Netherlands, 2017; Volume 4, pp. 660–667.
10. Azizi, S.; Mohamad, R.; Bahadoran, A.; Bayat, S.; Rahim, R.A.; Ariff, A.; Saad, W.Z. Effect of annealing temperature on antimicrobial and structural properties of bio-synthesized zinc oxide nanoparticles using flower extract of Anchusa italica. J.Photochem. Photobiol. B Biol. 2016, 161, 441–449.
11. Anbuvannan, M.; Ramesh, M.; Viruthagiri, G.; Shanmugam, N.; Kannadasan, N. Anisochilus carnosus leaf extract mediated synthesis of zinc oxide nanoparticles for antibacterial and photocatalytic activities. Mater. Sci. Semicond. Process. 2015, 39, 621–628.
12. Elumalai, K.; Velmurugan, S. Green synthesis, characterization and antimicrobial activities of zinc oxide nanoparticles from the leaf extract of Azadirachta indica (L.). Appl. Surf. Sci. 2015, 345, 329–336.
13. Supraja, N.; Prasad, T.N.V.K.V.; Krishna, T.G.; David, E. Synthesis, characterization, and evaluation of the antimicrobial efficacy of Boswellia ovalifoliolata stem bark-extract-mediated zinc oxide nanoparticles. Appl. Nanosci. 2016, 6, 581–590.
14. Singh, R.P. Biological Approach of Zinc Oxide Nanoparticles Formation and Its Characterization. Adv. Mater. Lett. 2011, 2,313–317.
15. Suresh, D.; Nethravathi, P.; Udayabhanu; Rajanaika, H.; Nagabhushana, H.; Sharma, S. Green synthesis of multifunctional zinc oxide (ZnO) nanoparticles using Cassia fistula plant extract and their photodegradative, antioxidant and antibacterial activities. Mater. Sci. Semicond. Process. 2015, 31, 446–454.
16. Habib S, Rashid F, Tahir H, Liaqat I, Latif AA, Naseem S, ... Jefri OA (2023) Antibacterial and cytotoxic effects of biosynthesized zinc oxide and titanium dioxide nanoparticles. Microorganisms 11(6):1363.
17. Archana P, Janarthanan B, Bhuvana S, Rajiv P, Sharmila S (2022) Concert of zinc oxide nanoparticles synthesized using Cucumis melo by green synthesis and the antibacterial activity on pathogenic bacteria. Inorg Chem Commun 137:109255.
18. Faisal S, Jan H, Shah SA, Shah S, Khan A, Akbar MT, ... Syed S (2021) Green synthesis of zinc oxide (ZnO) nanoparticles using aqueous fruit extracts of Myristica fragrans: Their characterizations and biological and environmental applications. ACS Omega 6(14):9709–9722.
19. Hoseinzadeh E, Alikhani MY, Samarghandi MR, Shirzad-Siboni M (2014) Antimicrobial potential of synthesized zinc oxide nanoparticles against gram positive and gram-negative bacteria. Desalin Water Treat 52(25–27):4969–4976.
20. Archana P, Janarthanan B, Bhuvana S, Rajiv P, Sharmila S (2022) Concert of zinc oxide nanoparticles synthesized using Cucumis melo by green synthesis and the antibacterial activity on pathogenic bacteria. Inorg Chem Commun 137:109255.